JOURNAL OF BACTERIOLOGY, June 2007, p. 4108–4119 Vol. 189, No. 11
0021-9193/07/$08.00+0 doi:10.1128/JB.00047-07

Insights into the Autotrophic CO_2 Fixation Pathway of the Archaeon *Ignicoccus hospitalis*: Comprehensive Analysis of the Central Carbon Metabolism▽

Ulrike Jahn,[1] Harald Huber,[1]* Wolfgang Eisenreich,[2] Michael Hügler,[3]§ and Georg Fuchs[3]*

Lehrstuhl Mikrobiologie und Archaeenzentrum, Universität Regensburg, Universitätsstr. 31, D-93053 Regensburg, Germany[1]; Lehrstuhl für Organische Chemie und Biochemie, Technische Universität München, Lichtenbergstr. 4, D-85748 Garching, Germany[2]; and Mikrobiologie, Fakultät Biologie, Universität Freiburg, Schänzlestr. 1, D-79104 Freiburg, Germany[3]

Received 10 January 2007/Accepted 19 March 2007

***Ignicoccus hospitalis* is an autotrophic hyperthermophilic archaeon that serves as a host for another parasitic/symbiotic archaeon, *Nanoarchaeum equitans*. In this study, the biosynthetic pathways of *I. hospitalis* were investigated by in vitro enzymatic analyses, in vivo ^{13}C-labeling experiments, and genomic analyses. Our results suggest the operation of a so far unknown pathway of autotrophic CO_2 fixation that starts from acetyl-coenzyme A (CoA). The cyclic regeneration of acetyl-CoA, the primary CO_2 acceptor molecule, has not been clarified yet. In essence, acetyl-CoA is converted into pyruvate via reductive carboxylation by pyruvate-ferredoxin oxidoreductase. Pyruvate-water dikinase converts pyruvate into phosphoenolpyruvate (PEP), which is carboxylated to oxaloacetate by PEP carboxylase. An incomplete citric acid cycle is operating: citrate is synthesized from oxaloacetate and acetyl-CoA by a (re)-specific citrate synthase, whereas a 2-oxoglutarate-oxidizing enzyme is lacking. Further investigations revealed that several special biosynthetic pathways that have recently been described for various archaea are operating. Isoleucine is synthesized via the uncommon citramalate pathway and lysine via the α-aminoadipate pathway. Gluconeogenesis is achieved via a reverse Embden-Meyerhof pathway using a novel type of fructose 1,6-bisphosphate aldolase. Pentosephosphates are formed from hexosephosphates via the suggested ribulose-monophosphate pathway, whereby formaldehyde is released from C-1 of hexose. The organism may not contain any sugar-metabolizing pathway. This comprehensive analysis of the central carbon metabolism of *I. hospitalis* revealed further evidence for the unexpected and unexplored diversity of metabolic pathways within the (hyperthermophilic) archaea.**

Ignicoccus hospitalis is a recently described member of the crenarchaeal order *Desulfurococcales* (38). Like the two other described *Ignicoccus* species, *Ignicoccus islandicus* and *Ignicoccus pacificus* (24), it is a strictly anaerobic, hyperthermophilic archaeon with an optimal growth temperature of 90°C. All *Ignicoccus* species grow chemolithoautotrophically, using the reduction of elemental sulfur with molecular hydrogen as the sole energy source and CO_2 as the sole carbon source. They possess a unique ultrastructure of the cell envelope with an outer membrane resembling that of gram-negative bacteria (40). Despite the great similarities, *I. hospitalis* shows a unique feature: it is the only known host of *Nanoarchaeum equitans*, a representative of the archaeal kingdom *Nanoarchaeota*. The two organisms represent the only known purely archaeal host-parasite system (25). As the smallest archaeal genome of *N. equitans* (490 kbp) lacks nearly all genes for biosynthetic pathways (48), it is likely that *I. hospitalis* provides all essential biosynthetic building blocks, like lipids or amino acids, for *N. equitans* (32).

The genome of *I. hospitalis* has also been sequenced (http://genome.jgi-psf.org/draft_microbes/ign_k/ign_k.draft.html). It is the second smallest archaeal genome known and exhibits only 1,434 putative genes, clearly indicating a high metabolic specialization of *I. hospitalis*. To maintain a continuous supply of organic carbon, *I. hospitalis* assimilates CO_2 into low-molecular-weight building blocks for biosynthesis. At present, four pathways of CO_2 fixation are known: the Calvin-Bassham-Benson cycle, the reductive citric acid cycle, the reductive acetyl-coenzyme A (CoA) pathway, and the 3-hydroxpropionate cycle, with a modified version present in the crenarchaeal order *Sulfolobales* (34). Preliminary experiments with *I. pacificus* and *I. islandicus* indicated that these autotrophic members of the *Desulfurococcales* lack the key enzymes of all these autotrophic pathways (28), raising the question of whether the members of the genus *Ignicoccus* use a new or modified pathway of autotrophic CO_2 fixation.

Another central biosynthetic process is gluconeogenesis. It is believed that gluconeogenesis in *Bacteria* and *Archaea* is achieved by the reversed Embden-Meyerhof pathway; in contrast to a rather uniform gluconeogenetic pathway, *Archaea* use an amazing variety of different pathways for glycolysis (44). The biosynthesis of pentose phosphate in *Archaea* is still an open question. Three possibilities for biosynthesis of pentoses have been described. The oxidative pentose phosphate pathway is mainly restricted to bacteria, whereas the nonoxidative

* Corresponding author. Mailing address for H. Huber: Lehrstuhl Mikrobiologie und Archaeenzentrum, Universität Regensburg, Universitätsstrasse 31, D-93053 Regensburg, Germany. Phone: 49 941 9433185. Fax: 49 941 9432403. E-mail: Harald.huber@biologie.uni-regensburg.de. Mailing address for G. Fuchs: Mikrobiologie, Biologie, Schaenzlestrasse 1, D-79104 Freiburg, Germany. Phone: 49 761 2032649. Fax: 9 761 2032626. E-mail: georg.fuchs@biologie.uni-freiburg.de.

§ Present address: Leibniz-Institut für Meereswissenschaften, IFM-GEOMAR, Kiel, Germany.

▽ Published ahead of print on 30 March 2007.

pentose phosphate pathway was found in several methanogens on the basis of enzymatic and genomic analyses (43, 50). In archaea lacking the genes for the nonoxidative or the oxidative pentose phosphate pathway, the ribulose-monophosphate pathway was recently suggested as an alternative for pentose phosphate biosynthesis, on the basis of genome analyses. In this pathway, pentose phosphate is synthesized by the release of formaldehyde from 3-hexulose 6-phosphate (13, 33, 45).

In this work, we investigated the autotrophic CO_2 fixation pathway of *I. hospitalis* and the biosynthesis of representative main cellular building blocks. Enzymatic analyses in vitro were combined with retrobiosynthetic analyses of in vivo ^{13}C-labeled amino acids. The experimental data were compared to the genome data of *I. hospitalis* to obtain comprehensive insight into the central metabolism in the organism. We suggest that *I. hospitalis* uses a novel, so far unknown pathway of CO_2 fixation.

MATERIALS AND METHODS

Strains and culture conditions. *I. hospitalis* strain KIN4/I^T was obtained from our culture collection and grown in synthetic-seawater medium, pH 5.5 (26), under a gas phase of H_2-CO_2 (80%/20% [vol/vol]) at 90°C. *Metallosphaera sedula* strain TH2^T (for control experiments) was grown autotrophically as described previously (27).

Production of ^{13}C-labeled cell masses. *I. hospitalis* cells were cultivated under autotrophic growth conditions in a 100-liter enamel-protected fermentor in the presence of 0.5 mM [1-^{13}C]acetate (Euriso-Top, Gif sur Yvette Cedex, France) (stirring, 150 rpm; gas phase, 300 kPa without gassing).

Incorporation of organic compounds. The incorporation of organic compounds into *I. hospitalis* cells was investigated by adding a mixture of unlabeled and ^{14}C-labeled compounds to the growth medium. [1-^{14}C]acetate (2.0 GBq mmol^{-1}; Amersham Biosciences, Freiburg, Germany), [3-^{14}C]pyruvate (0.6 GBq mmol^{-1}; American Radiolabeled Chemicals, St. Louis, MO), [1,4-^{14}C]succinate (2.0 GBq mmol^{-1}; American Radiolabeled Chemicals, St. Louis, MO), or [U-^{14}C]glucose (11.7 GBq mmol^{-1}; American Radiolabeled Chemicals, St. Louis, MO), respectively, was added (630, 140, 140, and 165 kBq, respectively, total radioactivity in a final concentration of 0.5 mM). Cells were grown in 1-liter serum bottles containing 250 ml medium under a gas pressure of 160 kPa (H_2-CO_2; 80/20) at 100 rpm. Samples (50 ml) were retrieved at intervals of 100 to 120 min during the exponential growth phase. The cell concentration was determined by cell counting using a Neubauer counting chamber. After a centrifugation step (40,000 × *g*; 30 min), the cells were washed with medium lacking the organic substrate and resuspended in 100 μl of fresh synthetic-seawater medium. Radioactivity was determined within this sample, as well as in 100 and 200 μl of the supernatant, by liquid scintillation counting.

Determination of the protein content of *I. hospitalis* cells. Cells grown in 20 ml culture medium to about 10^7 cells ml^{-1} (total, 2×10^8 cells) were harvested, washed, and resuspended in 1 ml of double-distilled water. The cells were lysed by 30-s ultrasonic treatment of the suspension (Sonifier 250; Branson, Danbury, CT). The protein content of the sample was determined to be 6 μg per 10^7 cells using the method of Bradford (5).

Syntheses. Malonyl-CoA, succinyl-CoA, acetyl-CoA, propionyl-CoA, L-malyl-CoA, and 3-hydroxypropionate were synthesized as described elsewhere (21), and the dry powders of the CoA esters were stored at −20°C.

Preparation of cell extracts. Cell extracts were prepared using a mixer mill (type MM2; Retsch, Haan, Germany); 0.5 ml buffer (100 mM Tris-HCl, pH 7.8, 3 mM 1,4-dithioerythritol [DTE], and 0.1 mg of DNase I per ml of buffer) and 0.5 g glass beads (diameter, 0.1 to 0.25 mm) were added to 0.1 g of wet cells in 1-ml stoppered glass vials in the anaerobic chamber. The solution was treated in the mixer mill for 6 min at 100% intensity (30 Hz). Following a centrifugation step (10 min; 12,000 × *g*; 4°C), the supernatant was used for enzyme tests. For larger amounts of cell extract, the cell suspension was passed through a French pressure cell at 137 MPa, and the lysate was ultracentrifuged (1 h; 100,000 × *g*; 4°C). The protein concentration in cell extracts was determined by the method of Bradford (5), using bovine serum albumin as a standard.

Enzyme assays. Routine enzyme assays (0.5 ml assay mixture) were performed in stoppered 0.5-ml glass cuvettes or 1-ml glass vials. For practical reasons, unless otherwise stated, the assay temperature was 75°C or 85°C, as specified in Results (compared to a 90°C growth temperature).

Assays with NADH, NADPH, NAD, or NADP. Reactions involving pyridine nucleotides were followed spectrophotometrically at 365 nm {$\varepsilon_{365\ nm}$[NAD(P)H] = 3.4×10^3 M^{-1} cm^{-1}}.

ATP citrate lyase, malate dehydrogenase, isocitrate dehydrogenase, aconitase, pyruvate kinase, 2-oxoglutarate dehydrogenase, and pyruvate dehydrogenase, as well as the reduction of malonyl-CoA to 3-hydroxypropionate and the reduction of 3-hydroxypropionate to propionyl-CoA, were measured as described previously (28). Isocitrate dehydrogenase and aconitase were tested under oxic and anoxic conditions.

For glyceraldehyde 3-phosphate dehydrogenase, the phosphate- and glyceraldehyde 3-phosphate-dependent reduction of NAD(P)$^+$ was monitored. The assay mixture (adjusted to pH 7.8) contained 100 mM Tris-HCl, 100 mM K_2HPO_4, 2 mM NAD(P)$^+$, and 3 mM glyceraldehyde 3-phosphate. The addition of glyceraldehyde 3-phosphate started the reaction. The presence of phosphate-independent glyceraldehyde 3-phosphate dehydrogenase was tested in an assay lacking phosphate.

Assays with viologen dyes. Reactions involving methyl viologen (MV) or benzyl viologen (BV) were followed spectrophotometrically at 578 nm [ε_{578} (MV) = 9.8×10^3 M^{-1} cm^{-1}; ε_{578} (BV) = 8.6×10^3 M^{-1} cm^{-1}] (7). The following anoxic assay mixture was used with N_2 gas as the headspace: 100 mM Tris-HCl, pH 7.8, 4 mM DTE, 2 mM $MgCl_2$, and 4 mM MV or 2 mM BV. Dithionite was added by syringe from 5 mM stock solution until a permanent faint bluish color was obtained.

For 2-oxoglutarate– and pyruvate-acceptor oxidoreductases, the assay mixture contained buffer, 1 mM CoA, and 3 mM 2-oxoglutarate or pyruvate. The reaction was started by the addition of 2-oxoglutarate or pyruvate. As a control, the assays were repeated by adding 0.5 mM thiamine-diphosphate to the reaction mixture.

For formate dehydrogenase, the assay mixture contained buffer and 3 mM formate; the reaction was started by the addition of formate.

For fumarate reductase, before the reaction was started, MV was reduced to an optical density at 578 nm of about 2.0 with dithionite. The addition of fumarate started the reaction.

Carbon monoxide dehydrogenase was measured according to a previously described method (30).

Other spectrophotometric assays. L-Malyl-CoA lyase, isocitrate lyase, fumarate hydratase, and citrate synthase were measured as described by Hügler et al. (28). All enzyme activities were tested under oxic and anoxic conditions.

Radioactive assays. Carboxylation reactions with $^{14}CO_2$ were followed by measuring the substrate-dependent incorporation of ^{14}C from [^{14}C]-bicarbonate into acid-stable products.

Ribulose 1,5-bisphosphate carboxylase/oxygenase (RubisCO), acetyl-CoA carboxylase, propionyl-CoA carboxylase, phosphoenolpyruvate (PEP) carboxylase, pyruvate carboxylase, PEP carboxykinase, pyruvate water dikinase (PEP synthase), and pyruvate phosphate dikinase were measured according to the method of Hügler et al. (28).

For 2-oxoglutarate– and pyruvate-acceptor oxidoreductases, the exchange of $^{14}CO_2$ into the carboxyl group of the 2-oxoacids in the absence of electron acceptors is characteristic of reversible 2-oxoacid synthases. The following anoxic assay mixture was used with N_2 gas as the headspace: 100 mM Tris-HCl, pH 7.8, 4 mM DTE, 2 mM $MgCl_2$, 10 mM $NaHCO_3$, 37 kBq [^{14}C]Na_2CO_3 (specific radioactivity, 2.5 Bq nmol^{-1}), and 3 mM 2-oxoglutarate or pyruvate. In some experiments, 1 mM CoA or 0.5 mM thiamine PP_i was included, but without effect. The reaction was started by the addition of 2-oxoglutarate or pyruvate.

Enzymatic assays coupled to phosphate determination. Reactions resulting in a substrate-dependent release of inorganic phosphate from the phosphorylated substrates were followed by measuring the substrate- and cell extract-dependent increase of inorganic phosphate in the assay (total volume, 0.25 ml). The buffer contained 100 mM Tris-HCl, pH 7.8, and 5 mM $MgCl_2$. Reaction mixtures were incubated at 85°C for 0, 2, and 5 min and stopped by rapid cooling on ice. Experiments in which substrate or cell extract, respectively, were omitted served as blanks and controls.

For fructose 1,6-bisphosphate phosphatase, the reaction was started by the addition of 4 mM fructose 1,6-bisphosphate to the reaction mixture.

For fructose 1,6-bisphosphate aldolase, the enzyme activity was determined in the direction of fructose bisphosphate formation by coupling the reaction to endogenous fructose 1,6-bisphosphate phosphatase activity, which dephosphorylates fructose 1,6-bisphosphate. Glyceraldehyde 3-phosphate (8 mM) was incubated for 10 min at 25°C in the presence of 5 U triosephosphate isomerase. Afterward, the assay mixture was heated to 85°C and the test was started by the addition of cell extract. The release of inorganic phosphate from fructose 1,6-bisphosphate was monitored.

The glyceraldehyde-3-phosphate dehydrogenase and phosphoglycerate kinase assay detected both activities, although the specific activity observed was that of the rate-limiting step. The NAD(P)H- and 3-phosphoglycerate-dependent release of inorganic phosphate from MgATP was followed. The reaction was coupled to the endogenous phosphoglycerate kinase activity, which forms 1,3-bisphosphoglycerate from 3-phosphoglycerate and ATP. The reaction mixture contained 0.5 mM NAD(P)H, 5 mM ATP, and 5 mM 3-phosphoglycerate. The reaction was started by the addition of 3-phosphoglycerate. The blank reaction in the absence of ATP was zero, and the blank value obtained in the presence of ATP and in the absence of NAD(P)H (20 nmol min^{-1} mg^{-1}) was subtracted from the measured values.

Determination of acid-stable ^{14}C. The fixation of ^{14}C from [^{14}C]bicarbonate into nonvolatile, acid-stable products was measured in samples (0.1 ml) incubated for 1, 5, and 10 min (see above). The addition of 20 μl of 6 M HCl (to pH 1 to 2) stopped the reaction. Volatile $^{14}CO_2$ (nonfixed) was removed by vigorously shaking the sample in open scintillation vials for 3 h. The remaining radioactivity in the liquid sample was then determined. The radioactivities in samples of two control experiments, in which the substrate and extract, respectively, were omitted, served as blanks and controls.

Determination of ^{14}C. The amount of ^{14}C in liquid samples (up to 0.2 ml) was determined by liquid scintillation counting using 3 ml of Rotiszint eco plus scintillation cocktail (Roth, Karlsruhe, Germany). The counting efficiency (75 to 85%) was determined via the channel ratio method.

Determination of inorganic phosphate. Inorganic phosphate released in enzymatic assays was determined using the modified malachite green-ammonium molybdate assay (22).

Detection of biotinylated proteins. Biotinylated proteins in cell extracts were detected with peroxidase-conjugated avidin as described previously (12, 35).

Fractionation of cell material. Cells (3 g [wet weight]) were suspended in 3 ml double-distilled water, and the suspension was treated with a sonifier (Sonifier 250; Branson, Danbury, CT). After cell disruption, 3 ml of 70% (vol/vol) $HClO_4$ was added to precipitate the protein. After 30 min of incubation on ice, a centrifugation step (15 min; 48,000 × *g*; 4°C) followed. To remove low-molecular-weight substances, the resulting pellet was washed three times with 10 ml 0.5 M $HClO_4$, followed by centrifugation (5 min; 48,000 × *g*). To extract nucleic acids, 10 ml 0.5 M $HClO_4$ was added to the pellet, and the solution was incubated at 70°C for 20 min. After centrifugation (15 min; 20,000 × *g*; 4°C), nucleic acids stayed in the supernatant and proteins in the pellet. To extract lipids, the pellet was resuspended in a mixture of ethanol and diethylether (3:1 [vol/vol]) and incubated at 40°C for 1 h. A centrifugation step (15 min; 20,000 × *g*; 4°C) separated the protein pellet from lipids in the supernatant. After a wash with 10 ml diethylether and centrifugation (15 min; 20,000 × *g*; 4°C), the protein pellet was dried by lyophilization (Celvinator Beta 1-16; Christ, Osterode, Germany). For protein hydrolysis, 3 ml 6 M HCl was added to the protein pellet. The suspension was incubated in sealed and evacuated glass ampoules at 112°C for 24 h. HCl was removed by three evaporation cycles, with the addition of 20 ml of double-distilled water after each cycle.

Separation of amino acids. Amino acids were isolated by chromatographic procedures, as described previously (10).

NMR spectroscopy. ^1H and ^{13}C nuclear magnetic resonance (NMR) spectra were recorded at 500.13 and 125.76 MHz, respectively, with a DRX500 spectrometer (Bruker Biospin, Rheinstetten, Germany) as described previously (9). Tyr and Asp were dissolved in D_2O containing 0.1 M NaOD (pH 13); the other amino acids were dissolved in D_2O containing 0.1 M DCl (pH 1). ^{13}C enrichments were determined for individual positions by quantitative NMR spectroscopy (9). Briefly, ^{13}C NMR spectra of the ^{13}C-labeled compound under study and of natural-abundance material were recorded under the same experimental conditions. Integrals were determined for each ^{13}C NMR signal, and the signal integral for each carbon atom in the labeled compound was referenced to that of the natural-abundance material, thus affording relative ^{13}C abundances for each position in the labeled molecular species. Relative abundances were normalized by assigning a value of 1.1% to the carbon atom with the lowest ^{13}C enrichment. The validity of this approach was confirmed for certain amino acids by analysis of ^{13}C coupling satellites in ^1H NMR spectra.

Database search. The genome sequence of *I. hospitalis* was obtained from http://genome.jgi-psf.org/draft_microbes/ign_k/ign_k.draft.html. Blast searches for genes encoding metabolic enzymes were performed using the program Clone Manager (Scientific & Educational Software). Query sequences were obtained from the Entrez gene database (http://www.ncbi.nlm.nih.gov/entrez/query.fcgi?CMD=search&DB=gene).

RESULTS

Search for key enzymes of autotrophic pathways. Cell extracts of *I. hospitalis* were screened for the presence of enzyme activities that were considered representative of the four known autotrophic CO_2 fixation pathways. Autotrophic growth under optimal conditions (90°C; pH 6.0; 1% S^0; H_2/CO_2 ratio, 80%/20% [vol/vol] at 250 kPa) occurred at a generation time of 1 h, corresponding to a specific growth rate (μ) of 0.011 min^{-1}. The cells that were studied grew with a generation time of approximately 2 h. Assuming a carbon content of 50% of the dry cell mass, the rate of carbon fixation under these conditions amounted to 0.4 μmol CO_2 fixed per min per mg of protein. This estimate is based on the specific substrate (S) consumption (*dS*) per time unit (*dt*): $dS/dt = (\mu/Y)X$, where *Y* represents the growth yield (1 g of dry cell mass formed per 0.5 g of carbon fixed) and *X* represents the cell dry mass in g (1 g of cell dry mass, corresponding to approximately 0.5 g of protein).

The activity of RubisCo, the key enzyme of the Calvin cycle, was tested as ribulose 1,5-bisphosphate-dependent fixation of $^{14}CO_2$ into acid-stable products. The specific activity at 80°C was below 1 nmol min^{-1} mg $protein^{-1}$, indicating that the Calvin cycle was not operating. Also, neither carbon monoxide dehydrogenase nor formate dehydrogenase activity—enzyme activities characteristic of the reductive acetyl-CoA pathway—was detectable (both were tested with MV as the artificial electron acceptor), indicating that the reductive acetyl-CoA pathway was not present, either.

In members of the *Sulfolobales*, acetyl-CoA/propionyl-CoA carboxylase is considered a key enzyme of a modified 3-hydroxypropionate cycle (28). Therefore, cell extracts were tested for the acetyl-CoA- or propionyl-CoA- plus Mg-ATP-dependent fixation of $^{14}CO_2$ into acid-stable products, but no activity was detected at 80°C. In addition, no malonyl-CoA reductase or propionyl-CoA synthase activity could be detected (<1 nmol min^{-1} mg $protein^{-1}$). These enzymes are characteristic of the 3-hydroxypropionate cycle in *Chloroflexus aurantiacus*, and their activities could also be measured in *Sulfolobales* (1, 2, 28, 29, 31a). The presence of biotin proteins, such as the biotin carrier protein of acetyl-CoA carboxylase or pyruvate carboxylase, was investigated using the avidin technique. Extracts of *I. hospitalis* showed no detectable biotin-containing protein, whereas the small 18.6-kDa biotin carrier protein of acetyl-CoA/propionyl-CoA carboxylase in *M. sedula* extract, which served as a positive control, stained extremely strongly (not shown). Also, no band with a molecular mass around 65 kDa was visible. This would be the approximate size of the biotin-containing subunit of pyruvate carboxylase (e.g., in *Methanocaldococcus jannaschii* or *Mycobacterium smegmatis*, (36, 37). These results exclude the operation of a 3-hydroxypropionate cycle.

Members of the *Thermoproteales* exhibit a reductive citric acid cycle for autotrophic CO_2 fixation. Cell extracts of *I. hospitalis* did not catalyze the 2-oxoglutarate- and CoA-dependent reduction of viologen dyes or the exchange of $^{14}CO_2$ into 2-oxoglutarate in the presence or absence of CoA (<1 nmol min^{-1} mg $protein^{-1}$ at 75°C or 85°C), which is characteristic of 2-oxoglutarate–acceptor oxidoreductase, a key enzyme of this cycle. Since pyruvate-acceptor oxidoreductase activity was clearly detectable by the same methods (see below), the failure

TABLE 1. Specific activities of enzymes of the central carbon metabolism in *I. hospitalis*

Enzyme	EC no.	No. of putative gene[a]	Incubation temp (°C)	Sp act (nmol min^{-1} mg $protein^{-1}$)
Citrate synthase	2.3.3.1 2.3.3.3	NF	75	21 ± 4
ATP citrate lyase	2.3.3.8	NF	75	<1
Aconitase	4.2.1.3	NF	75	31 ± 2
Isocitrate dehydrogenase ($NADP^+$)	1.1.1.42	1027	75	240 ± 20
2-Oxoglutarate dehydrogenase ($NADP^+$ NAD^+)	1.2.1.52	NF	75	<1
2-Oxoglutarate–acceptor oxidoreductase	1.2.7.3	NF[b]		
MV			75	<1
$^{14}CO_2$ exchange			85	<1
Fumarate hydratase (class I)	4.2.1.2	658	75	895 ± 45
Fumarate reductase (MV)	1.3.99.1	145	75	840 ± 130
Malate dehydrogenase		1223		
NAD^+	1.1.1.37		75	1,190 ± 240
$NAPD^+$	1.1.1.82		75	745 ± 100
Malyl-CoA lyase	4.1.3.24	NF	75	<1
Pyruvate dehydrogenase (NAD^+ $NADP^+$)	1.2.1.51	NF	75	<1
Pyruvate-acceptor oxidoreductase	1.2.7.1	1217–1220		
MV			75	115 ± 15
$^{14}CO_2$ exchange			85	145 ± 15
Pyruvate carboxylase	6.4.1.1	NF	85	<1
Pyruvate kinase	2.7.1.40	NF	85	<1
Pyruvate-phosphate dikinase	2.7.9.1	NF	85	<1
Pyruvate-water dikinase	2.7.9.2	1075	85	210 ± 10
PEP carboxylase	4.1.1.31	Present, gene not annotated	85	202 ± 20
PEP carboxykinase	4.1.1.32	NF	85	<1
PEP carboxytransphosphorylase	4.1.1.38	NF	85	<1
Lactate dehydrogenase (L-LDH, NAD^+)	1.1.1.27	NF	75	<1
Lactate dehydrogenase (D-LDH, NAD^+)	1.1.1.28			
Fructose 1,6-bisphosphatase	3.1.3.11	Present, gene not annotated	85	146 ± 4
Fructose 1,6-bisphosphate aldolase	4.1.2.13	NF	85	116 ± 16
Glyceraldehyde 3-phosphate dehydrogenase	1.2.1.12	967	75	
NADH				106 ± 10
NADPH				270 ± 10

[a] Derived from http://genome.jgi-psf.org/draft_microbes/ign_k/ign_k.draft.html. NF, not found.
[b] Two copies of genes coding for 2-oxoacid–acceptor oxidoreductases are present in the genome, one of which must definitely code for pyruvate-acceptor oxidoreductase. The function of the other is unknown.

to detect 2-oxoglutarate–acceptor oxidoreductase was not due to experimental failure but was most likely due to the absence of this enzyme of the reductive citric acid cycle. In addition, ATP citrate lyase activity was not detectable (<1 nmol min^{-1} mg $protein^{-1}$ at 75°C), excluding the reductive citric acid cycle as a potential carbon fixation pathway.

In summary, no evidence for the operation of one of the known CO_2 fixation pathways was obtained. However, two possible CO_2-fixing enzyme activities were easily detected: pyruvate-acceptor oxidoreductase activity was observed both in the spectrophotometric assay with MV as the electron acceptor (115 ± 15 nmol min^{-1} mg $protein^{-1}$ at 75°C) and in the radioactive assay following the exchange of $^{14}CO_2$ into the carboxyl group (145 ± 15 nmol min^{-1} mg $protein^{-1}$ at 85°C). In contrast, no pyruvate dehydrogenase or 2-oxoglutarate dehydrogenase activity was observed with NAD^+ or $NADP^+$ as the electron acceptor (<1 nmol min^{-1} mg $protein^{-1}$ at 75°C). Furthermore, PEP carboxylase was present and highly active (202 ± 20 nmol min^{-1} mg $protein^{-1}$ at 85°C).

Enzyme activities in extracts of autotrophically grown cells. The presence of pyruvate-acceptor oxidoreductases suggests that acetyl-CoA is reductively carboxylated to pyruvate. Therefore, enzyme activities possibly involved in biosynthesis starting from pyruvate were investigated at 75°C or 85°C in cell extracts of *I. hospitalis*. The results of the measurement are presented in Table 1. Figure 1 gives an overview of the reactions involved.

Extracts catalyzed the PEP-dependent fixation of $^{14}CO_2$ into acid-stable products in the presence of NADH with a specific activity of 202 ± 20 nmol min^{-1} mg $protein^{-1}$. Phosphate, GDP, or ADP did not stimulate the reaction rate, excluding activities of PEP carboxytransphosphorylase (requiring phosphate) (PEP + P_i + HCO_3^- → oxaloacetate + PP_i) or PEP carboxykinase (requiring GDP or ADP) (PEP + ADP + HCO_3^- → oxaloacetate + ATP). These results suggest the presence of PEP carboxylase activity catalyzing the formation of oxaloacetate from PEP and CO_2 (PEP + HCO_3^- → oxaloacetate + P_i), which was coupled to the reduction of oxaloacetate by NADH-dependent malate dehydrogenase.

PEP formation from pyruvate was tested by coupling PEP conversion to malate catalyzed by endogenous PEP carboxylase and NADH-dependent malate dehydrogenase. Extracts fixed $^{14}CO_2$ in an Mg-ATP- and pyruvate-dependent reaction in the presence of NADH with a specific activity of 210 ± 10 nmol min^{-1} mg $protein^{-1}$. The addition of phosphate did not stimulate excluding the activity of pyruvate-phosphate dikinase (pyruvate + ATP + P_i → PEP + AMP + PP_i). The reaction

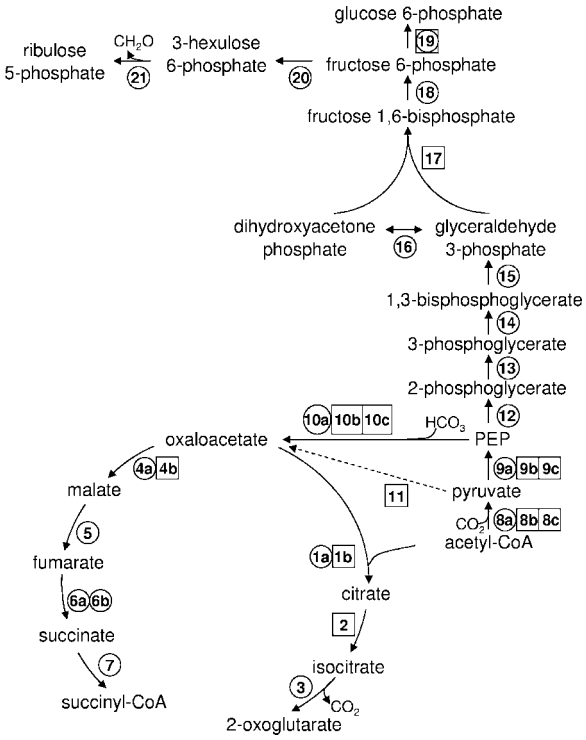

FIG. 1. Biosynthetic capacity of *I. hospitalis*, according to genome data. Circles, putative genes of enzymes that were detected (E value < e−11); squares, genes of enzymes that were not detected in the *I. hospitalis* genome. The numbers of the putative genes of the *I. hospitalis* genome are shown: 1a, citrate synthase; 1b, ATP citrate lyase; 2, aconitase; 3, isocitrate dehydrogenase; 4a, malate dehydrogenase; 4b, malate quinone oxidoreductase; 5, fumarate hydratase; 6a, fumarate reductase; 6b, succinate dehydrogenase; 7, succinate-CoA ligase (ADP forming); 8a, 2-oxoacid–ferredoxin oxidoreductase; 8b, acetyl-CoA carboxylase; 8c, pyruvate dehydrogenase; 9a, pyruvate-water dikinase; 9b, pyruvate-phosphate dikinase; 9c, pyruvate kinase; 10a, PEP carboxylase; 10b, PEP carboxykinase; 10c, PEP carboxytransphosphorylase; 11, pyruvate carboxylase; 12, enolase; 13, phosphoglycerate mutase; 14, phosphoglycerate kinase; 15, glyceraldehyde 3-phosphate dehydrogenase; 16, triosephosphate isomerase; 17, fructose 1,6-bisphosphate aldolase; 18, fructose 1,6-bisphosphate phosphatase; 19, phosphoglucose isomerase (cupin type); 20, 3-hexulose 6-phosphate isomerase; 21, 3-hexulose 6-phosphate synthase.

was also not inhibited by avidin, which excludes oxaloacetate formation via biotin-dependent pyruvate carboxylase (pyruvate + HCO_3^- + ATP → oxaloacetate + ADP + P_i). These results indicate the presence of pyruvate-water dikinase (PEP synthetase) (pyruvate + ATP + H_2O → PEP + AMP + P_i). Pyruvate kinase activity (PEP + ADP → pyruvate + ATP) could not be detected.

The level of $NAD(P)^+$-dependent malate dehydrogenase activity was high when oxaloacetate reduction with NADPH (745 ± 100 nmol min^{-1} mg $protein^{-1}$) and NADH (1,190 ± 240 nmol min^{-1} mg $protein^{-1}$) were tested. Fumarase activity, measured in the direction of fumarate hydration, was 895 ± 45 nmol min^{-1} mg $protein^{-1}$. Fumarate reductase activity tested with reduced MV as the electron donor was 840 ± 45 nmol min^{-1} mg $protein^{-1}$.

Extracts catalyzed the formation of citrate from oxaloacetate and acetyl-CoA with a specific activity of 21 ± 4 nmol min^{-1} mg $protein^{-1}$. This activity was oxygen sensitive and detectable only under anoxic conditions. Since ATP citrate lyase activity was not detectable (the observed reaction did not require ADP and phosphate), this indicates the presence of a citrate synthase. Aconitase activity turned out also to be oxygen sensitive (30 ± 2 nmol min^{-1} mg $protein^{-1}$). Isocitrate dehydrogenase was $NADP^+$ specific (238 ± 22 nmol min^{-1} mg^{-1}). As indicated above, both $NAD(P)^+$ dependent 2-oxoglutarate dehydrogenase and 2-oxoglutarate–acceptor oxidoreductase activities were lacking. L-Malyl-CoA lyase activity was not detected.

Characteristic enzymes of gluconeogenesis were found. 3-Phosphoglycerate kinase and glyceraldehyde 3-phosphate dehydrogenase activities were measured in one assay and were clearly present (270 ± 10 nmol min^{-1} mg $protein^{-1}$), with a preference of the dehydrogenase for NADPH. Similarly, fructose 1,6-bisphosphate aldolase and fructose 1,6-bisphosphate phosphatase were measured in one assay, and both enzymes were clearly detected (116 ± 16 nmol min^{-1} mg $protein^{-1}$ and 146 ± 4 nmol min^{-1} mg $protein^{-1}$, respectively, at 85°C).

Database search. The available genome database of *I. hospitalis* (http://genome.jgi-psf.org/draft_microbes/ign_k/ign_k.draft.html) was screened for the presence of putative genes coding for autotrophic pathways (Table 1). The results are summarized and visualized in Fig. 1.

Citric acid cycle. All putative genes for the citric acid cycle were detected, except for an (si)-specific citrate synthase and a 2-oxoglutarate dehydrogenase (Table 1). Probes for (si)-specific citrate synthase used for screening the database were from *Thermus aquaticus*, *Pyrococcus furiosus*, and *Escherichia coli*, but all E values were >e−5. However, since citrate synthase activity could be clearly detected, the gene encoding a putative (re)-specific citrate synthase must be present. Its gene is not known, and any annotation is therefore speculative. The genes for isocitrate lyase, L-malate synthase, L-malyl-CoA lyase, ATP citrate lyase, citrate lyase, and malic enzyme were not detected. The genes for succinate dehydrogenase were most similar to those of *Sulfolobus acidocaldarius*. However, it is unclear whether fumarate reduction is catalyzed by the annotated succinate dehydrogenase or by a separate fumarate reductase. It should be mentioned that two gene clusters containing the four subunits of putative 2-oxoacid–acceptor oxidoreductases were present. However, 2-oxoglutarate dehydrogenase or 2-oxoglutarate–acceptor oxidoreductase activity was not detectable, in contrast to pyruvate-acceptor oxidoreductase activity. These data taken together suggest the presence of an incomplete citric acid cycle that serves solely anabolic purposes. However, the nature of citrate synthase remains elusive.

Pyruvate and PEP synthesis and C-3 and C-4 interconversion. The putative genes for pyruvate-acceptor oxidoreductase (pyruvate synthase) were found; in contrast, pyruvate dehydrogenase genes were not found. Furthermore, a putative gene for pyruvate-water dikinase (PEP synthetase) that forms PEP was detected. The corresponding genes for pyruvate-phosphate dikinase or pyruvate kinase were not seen. The putative gene for PEP carboxylase was present. The alternative routes of oxaloacetate synthesis from pyruvate via pyruvate carboxylase, as well as PEP carboxykinase and PEP carboxytransphosphorylase, seem not to be present, since these genes were not detected. This suggests that acetyl-CoA is reductively carboxylated to pyruvate by pyruvate synthase and then converted to

TABLE 2. Incorporation rates of organic substrates into *I. hospitalis* cell carbon[a]

Labeled proffered compound (0.5 mM/250 ml growth medium)	Specific radioactivity of labeled proffered compound (dpm nmol^{-1})	Cells formed (μg protein ml^{-1})	^{14}C in cell pellet (dpm ml^{-1})	C in cell pellet from labeled proffered compound (μg ml^{-1})	% Cell carbon derived from labeled compound
[1-^{14}C]acetate (140 kBq)	68	5.4	1,782	0.629	11.6
[3-^{14}C]pyruvate (630 kBq)	300	7.2	5,127	0.615	8.5
[1,4-^{14}C]succinate (140 kBq)	68	5.4	670	0.473	8.8

[a] Calculated from the incorporation of ^{14}C-labeled compounds. Cells were harvested at a cell concentration of about 6×10^6 ml^{-1}.

PEP by PEP synthetase and that PEP then gives rise to oxaloacetate via PEP carboxylase.

Gluconeogenesis from PEP and pentosephosphate synthesis. Gluconeogenesis from PEP via fructose 1,6-bisphosphate and fructose 6-phosphate seems to proceed in the conventional way, with some remarkable exceptions regarding the nature of the enzymes. The putative genes coding for enolase, phosphoglycerate mutase, phosphoglycerate kinase, glyceraldehyde 3-phosphate dehydrogenase, and triosephosphate isomerase were found. A gene coding for fructose 1,6-bisphosphate aldolase was not detected. The same was true for the classical hexosephosphate isomerase. However, a 1-phosphoglucose isomerase of the cupin superfamily was found, although with only a low E value (e−11) for the corresponding gene from *Thermococcus litoralis*; this gene product is thought to act as hexosephosphate isomerase. A putative fructose 1,6-bisphosphate phosphatase gene was found. In contrast, the genes for the classical enzymes of the pentose phosphate pathway, glucose 6-phosphate dehydrogenase, 6-phosphogluconolactone hydrolase, and 6-phosphogluconate dehydrogenase, were lacking. Instead, the two genes for the enzymes of the recently proposed ribulose monophosphate pathway of pentosephosphate synthesis, 3-hexulose 6-phosphate isomerase and 3-hexulose 6-phosphate synthase, were present.

Glycolysis. Genes for enzymes of the nonphosphorylating or phosphorylating Entner-Doudoroff pathway could not be found. Also, the genes coding for glucokinase and phosphofructokinase of a (modified) Embden-Meyerhof pathway were not detected. The gene for pyruvate-kinase was also not detected. However, it should be mentioned that in *Archaea*, PEP synthase can function as pyruvate kinase, as well (31). The genes coding for glyceraldehyde 3-phosphate–ferredoxin oxidoreductase (EC 1.2.7.6) and nonphosphorylative NAD^+- or $NADP^+$-dependent glyceraldehyde 3-phosphate dehydrogenase (EC 1.2.1.9 or EC 1.2.1.12, respectively) were missing. However, the gene for $NAD(P)^+$-dependent phosphorylative D-glyceraldehyde 3-phosphate dehydrogenase (EC 1.2.1.59) was present (see above) and likely functions in gluconeogenesis.

Incorporation of ^{14}C-labeled acetate, pyruvate, succinate, and glucose. *I. hospitalis* was grown autotrophically under anaerobic conditions with hydrogen as the electron donor and elemental sulfur as the electron acceptor (25). To test the incorporation of organic substrates, ^{14}C-labeled acetate, pyruvate, succinate, or glucose was added to the medium at a concentration of 0.5 mM (Table 2). The generation time of *I. hospitalis* was about 60 min in all experiments, and cells were harvested at the end of the exponential growth phase. Figure 2 shows the accumulation of radioactivity from each labeled compound in the cell pellet and the decrease of radioactivity in the cell-free medium during growth. The organic compounds contributed to different extents to the cell material. Approximately 5.2% of the proffered labeled acetate, 3.5% of the pyruvate, 1.9% of the succinate, and 0% of the glucose were incorporated. In the experiments with pyruvate and succinate, losses of total radioactivity of 31% and 44%, respectively, occurred, which were most probably caused by the release of $^{14}CO_2$ produced from the labeled compounds.

Calculating the mass of carbon derived from the proffered organic compound and comparing it with the cell mass, acetate

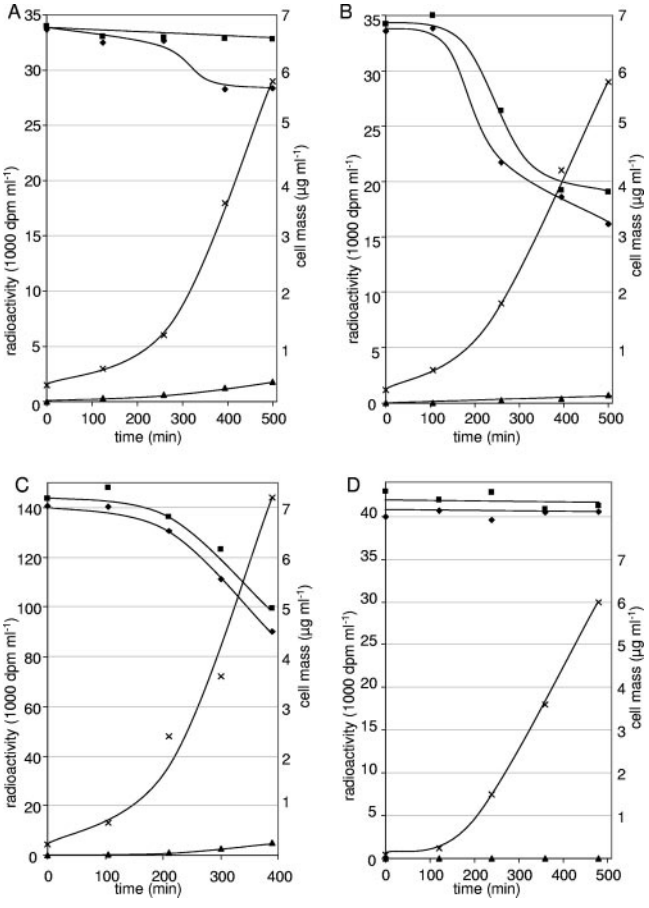

FIG. 2. Incorporation of ^{14}C-labeled substrates by growing *I. hospitalis* cells. (A) [1-^{14}C]acetate. (B) [1,4-^{14}C]succinate. (C) [3-^{14}C]pyruvate. (D) [U-^{14}C]glucose. The total radioactivities in the assay (■), in the supernatant/cell-free medium (◆), and in the cells (▲) in relation to the dry cell mass (×) of the growing *I. hospitalis* culture are shown.

TABLE 3. ^{13}C abundances of amino acids from *I. hospitalis* autotrophically grown in the presence of 0.5 mM [1-^{13}C]acetate

Amino acid	Position	Chemical shift δ (ppm)	Relative ^{13}C (%)	Corresponding position(s)[a]
Alanine	1	171.0	ND[b]	1 (pyruvate), CO_2
	2	50.7	16.8	2 (pyruvate), 1 (acetyl-CoA)
	3	17.8	3.3	3 (pyruvate), 2 (acetyl-CoA)
Serine	1	173.6	ND	1 (PEP)
	2	53.3	15.3	2 (PEP)
	3	57.9	3.3	3 (PEP)
Aspartate	1	180.7	1.1	1 (oxaloacetate), 1 (pyruvate), CO_2
	2	54.4	14.5	2 (oxaloacetate), 2 (pyruvate), 1 (acetyl-CoA)
	3	43.7	4.6	3 (oxaloacetate), 3 (pyruvate), 2 (acetyl-CoA)
	4	182.8	1.1	4 (oxaloacetate), CO_2
Threonine	1	ND	ND	1 (oxaloacetate), 1 (pyruvate), CO_2
	2	56.9	14.0	2 (oxaloacetate), 2 (pyruvate), 1 (acetyl-CoA)
	3	63.9	3.3	3 (oxaloacetate), 3 (pyruvate), 2 (acetyl-CoA)
	4	14.2	1.1	4 (oxaloacetate), CO_2
Isoleucine	1	171.6	18.1	1 (acetyl-CoA)
	2	57.6	2.2	2 (acetyl-CoA)
	3	39.1	14.9	2 (pyruvate), 1 (acetyl-CoA)
	4	24.9	6.2	2 (pyruvate), 1 (acetyl-CoA)
	5	11.4	1.1	3 (pyruvate), 2 (acetyl-CoA)
	6	14.5	1.3	3 (pyruvate), 2 (acetyl-CoA)
Glutamate	1	183.3	20.0	1 (oxoglutarate), 1 (acetyl-CoA)
	2	56.3	5.3	2 (oxoglutarate), 2 (acetyl-CoA)
	3	32.2	16.9	3 (oxoglutarate), 2 (oxaloacetate), 2 (pyruvate), 1 (acetyl-CoA)
	4	34.5	5.7	4 (oxoglutarate), 3 (oxaloacetate), 3 (pyruvate), 2 (acetyl-CoA)
	5	183.5	1.1	5 (oxoglutarate), 4 (oxaloacetate), CO_2
Proline	1	171.6	19.7	1 (oxoglutarate), 1 (acetyl-CoA)
	2	59.5	4.0	2 (oxoglutarate), 2 (acetyl-CoA)
	3	28.3	12.9	3 (oxoglutarate), 2 (oxaloacetate), 2 (pyruvate), 1 (acetyl-CoA)
	4	23.5	4.1	4 (oxoglutarate), 3 (oxaloacetate), 3 (pyruvate), 2 (acetyl-CoA)
	5	46.5	1.1	5 (oxoglutarate), 4 (oxaloacetate), CO_2
Arginine	1	170.0	11.0	1 (oxoglutarate), 1 (acetyl-CoA)
	2	50.8	6.7	2 (oxoglutarate), 2 (acetyl-CoA)
	3	25.3	14.5	3 (oxoglutarate), 2 (oxaloacetate), 2 (pyruvate), 1 (acetyl-CoA)
	4	22.2	5.2	4 (oxoglutarate), 3 (oxaloacetate), 3 (pyruvate), 2 (acetyl-CoA)
	5	38.8	1.1	5 (oxoglutarate), 4 (oxaloacetate), CO_2
	6	164.1	3.1	
Lysine	1	171.9	22.6	1 (acetyl-CoA)
	2	51.5	7.6	2 (acetyl-CoA)
	3	27.0	6.9	2 (oxoglutarate), 2 (acetyl-CoA)
	4	18.7	26.3	3 (oxoglutarate), 2 (oxaloacetate), 2 (pyruvate), 1 (acetyl-CoA)
	5	23.5	7.7	4 (oxoglutarate), 3 (oxaloaceate), 3 (pyruvate), 2 (acetyl-CoA)
	6	36.2	1.1	5 (oxoglutarate), 4 (oxaloacetate), CO_2
Histidine	1	165.5	3.1	5 (ribose 5-phosphate)
	2	51.6	13.5	4 (ribose 5-phosphate)
	3	21.3	1.1	3 (ribose 5-phosphate)
	4	134.1	2.4	2 (ribose 5-phosphate)
	5	118.2	15.0	1 (ribose 5-phosphate)
	6	146.1	1.3	
Phenyl-alanine	1	182.4	ND	1 (PEP)
	2	57.4	44	2 (PEP)
	3	40.7	4	3 (PEP)
	4	138.2	26.9	2 (PEP)
	5/9	129.4	2.6	3 (PEP)/4 (erythrose 4-phosphate)
	6/8	128.5	5.4	3/1 (erythrose 4-phosphate)
	7	126.6	1.1	2 (erythrose 4-phosphate)
Tyrosine	1	183.4	1.1	1 (PEP)
	2	57.9	43	2 (PEP)
	3	40.3	5	3 (PEP)
	4	123.6	22.7	2 (PEP)
	5/9	131.1	7.6	3 (PEP)/4 (erythrose 4-phosphate)
	6/8	119.1	9.9	3/1 (erythrose 4-phosphate)
	7	165.0	ND	2 (erythrose 4-phosphate)

[a] On the basis of the metabolic network in *I. hospitalis*, equivalent positions in the respective building blocks of the index amino acid are indicated.
[b] ND, not determined.

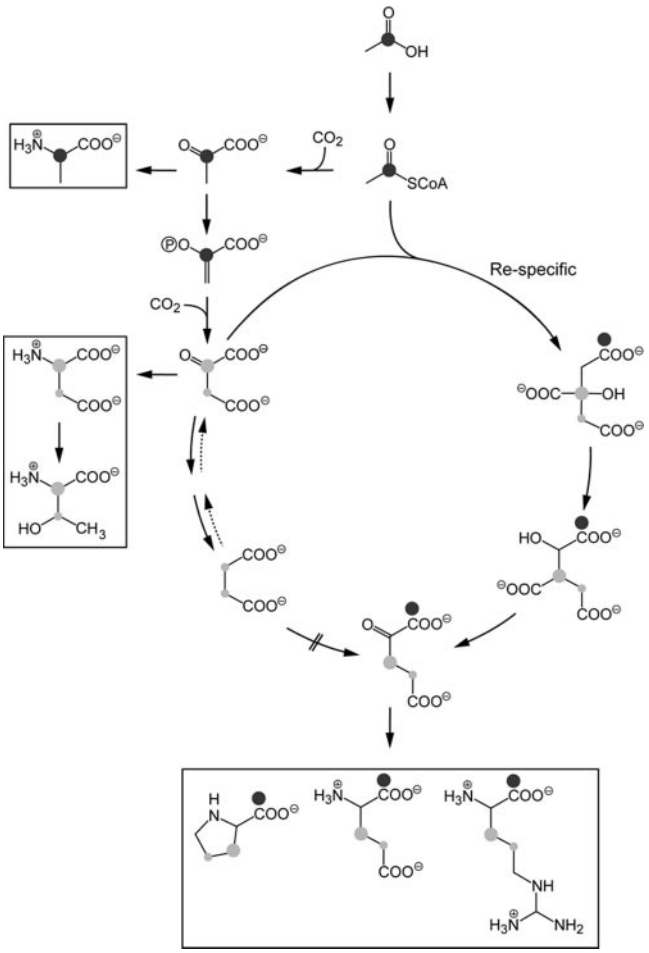

FIG. 3. Proposed incomplete pathway of CO_2 fixation in *I. hospitalis*. The proposed pathway was deduced from the labeling pattern and the complement of enzymes and genes of *I. hospitalis*. The circles represent highly ^{13}C-enriched carbon atoms from [1-^{13}C]acetate. Partial randomization of labeling in oxaloacetate is explained by reversible reactions between oxaloacetate, malate, fumarate, and succinate. A reductive carboxylation of succinyl-CoA implies a lack of ^{13}C enrichment at C-1 of 2-oxoglutarate. This is at odds with the labeling data for glutamate, proline, and arginine, which all display high ^{13}C enrichment at C-1. The compounds in boxes were analyzed.

contributed 11.6%, pyruvate 8.5%, and succinate 8.8% to the cell carbon (Table 2). Thus, the contribution of the proffered organic carbon to the cell carbon at the time of harvest of the cultures was ≤12% in all cases; the rest of the cell carbon should have been derived from CO_2. These values were calculated from the specific radioactivity of the total carbon of the proffered organic compounds, the amount of ^{14}C incorporated into the cell pellet, and the amount of protein formed, assuming 1 g of dry cell mass was equal to 0.5 g of cell protein or 0.5 g of cell carbon, respectively.

This obligate autotrophic archaeon, like other obligate autotrophic microorganisms, obviously is able to assimilate to a certain extent external carbon sources, such as acetate. Assimilation of acetate requires an acetate-activating enzyme, and the gene coding for an acetate-CoA ligase (AMP forming) was detected in the genome, whereas genes for acetate kinase and phosphotransacetylase were not found. Succinate and pyruvate assimilation do not need activation, and uptake may proceed by passive diffusion of the protonated form of the carboxylic acids. Glucose apparently was not taken up.

Labeling of growing cells with ^{13}C-labeled compounds and distribution of ^{13}C in individual building blocks. Cells were grown for at least six generations in the presence of 0.5 mM [1-^{13}C]acetate, and then amino acids were isolated from the protein fraction and the ^{13}C distributions in the individual carbon positions of the amino acids were determined by ^{13}C NMR spectroscopy (Table 3). The values indicate that in this experiment up to 20% of the basic building blocks of amino acids were derived from carbons of the exogenous acetate precursor.

The retrobiosynthetic approach allows a determination of the labeling pattern of intermediates of the central carbon metabolism from the amino acid patterns (3). For instance, the labeling pattern of alanine directly reflects the labeling pattern of its precursor molecule, pyruvate. Conversely, the labeling of the building blocks allows predictions as to the biosynthetic pathway, once the labeling pattern of central intermediates and the topology of the metabolic network have been deduced (Fig. 3 and Table 3). The averaged reconstructed ^{13}C distributions in the central intermediates, acetyl-CoA, pyruvate, oxaloacetate, 2-oxoglutarate, and ribose-5-phosphate, are given in Table 4.

Acetyl-CoA is the starting point of the postulated new autotrophic CO_2 fixation pathway. The dominant labeling of acetyl-CoA at C-1 reflects the labeling of the precursor molecule. C-2 was also weakly labeled, indicating either that the

TABLE 4. Rule-derived ^{13}C abundances in central metabolites of *I. hospitalis* autotrophically grown in the presence of 0.5 mM [1-^{13}C]acetate[a]

Metabolite	Position	% ^{13}C	Reconstructed and averaged from:
Acetyl-CoA	1	16.3 ± 4.9	Ala, Asp, Thr, Ile, Glu, Pro, Arg, Lys
	2	4.6 ± 2.1	Ala, Asp, Thr, Ile, Glu, Pro, Arg, Lys
Pyruvate	1	1.1	Asp
	2	15.2 ± 5.2	Ala, Asp, Thr, Ile, Glu, Pro, Arg, Lys
	3	4.0 ± 2.1	Ala, Asp, Thr, Ile, Glu, Pro, Arg, Lys
Oxaloacetate	1	1.1	Asp
	2	16.5 ± 4.9	Asp, Thr, Ile, Glu, Pro, Arg, Lys
	3	5.1 ± 1.5	Asp, Thr, Ile, Glu, Pro, Arg, Lys
	4	1.1 ± 0	Asp, Thr, Ile, Glu, Pro, Arg, Lys
2-Oxoglutarate	1	16.9 ± 5.1	Glu, Pro, Arg
	2	5.7 ± 1.3	Glu, Pro, Arg, Lys
	3	17.6 ± 5.9	Glu, Pro, Arg, Lys
	4	5.7 ± 1.5	Glu, Pro, Arg, Lys
	5	1.1 ± 0	Glu, Pro, Arg, Lys
Ribose 5-phosphate	1	15.0	His
	2	2.4	His
	3	1.1	His
	4	13.5	His
	5	3.1	His

[a] The data are reconstructed and averaged from isotopologue profiles in amino acids (cf. Table 3).

formation of acetyl-CoA from other intermediates was only marginal or that acetyl-CoA, the presumed CO_2 acceptor molecule and starting point of the postulated CO_2 fixation pathway, is re-formed in a cyclic process resulting again in a prominent label accumulation in C-1 rather than in C-2.

All of the data can be integrated into a hypothetical pathway of CO_2 fixation in *I. hospitalis* (Fig. 3) that is still incomplete. The labeling of pyruvate predominantly at C-2 is consistent with its synthesis from acetyl-CoA and CO_2 via pyruvate synthase. Oxaloacetate was strongly labeled at C-2, which is also consistent with its biosynthesis from pyruvate via PEP. The partial acquisition of label in C-3 is probably due to the randomization that occurs when oxaloacetate partly equilibrates with symmetric fumarate or succinate.

Interestingly, the labeling of 2-oxoglutarate preferentially at C-1 and C-3 is consistent with its synthesis via citrate and isocitrate involving a (re)-specific citrate synthase. The operation of a (si)-specific enzyme would result in the formation of C-3- and C-5-labeled 2-oxoglutarate. In any case, the reductive carboxylation of succinyl-CoA can be excluded, since a random labeling of C-3 and C-4 would be expected, and in no case should C-1 be labeled.

The labeling of ribose 5-phosphate preferentially at C-1 and C-4 (deduced from the labeling of histidine) indicates that hexose phosphate labeled at C-2 and C-5 was presumably an intermediate (the biosynthetic pathway is shown in Fig. 4). This pattern is consistent with the synthesis of fructose 1,6-bisphosphate from two molecules of C-2-labeled pyruvate via gluconeogenesis and conversion of hexosephosphate to pentosephosphate via the ribulose-monophosphate pathway (see "Special biosynthetic pathways" below).

Special biosynthetic pathways. Pentosephosphate may be formed by oxidation and loss of C-1 as CO_2 in the classical oxidative pentose phosphate pathway or via release of formaldehyde from C-1 in the novel archaeal ribulose monophosphate pathway (13, 33, 45) (Fig. 4). Due to the cleavage of C-1, both pathways lead to identical labeling patterns of the resulting pentosephosphates. However, the genome data suggest the operation of the ribulose-monophosphate pathway in *I. hospitalis*.

Biosynthesis of aromatic compounds may proceed either via the classical pathway that starts from erythrose 4-phosphate and PEP or via the novel pathway that starts from L-aspartate semialdehyde and 6-deoxy-5-keto-fructose-1-phosphate (49). Coincidentally, the labeling patterns that can be predicted to arise from [1-^{13}C]acetate via the two alternatives are very similar (Fig. 5). The apparent enrichment detected for the ortho ring positions in phenylalanine and tyrosine, albeit weak, might suggest the involvement of the aspartate semialdehyde pathway. In the genome, however, both genes for the initial two enzymes of the classical pathway, 3-deoxy-D-arabino-heptulosonate 7-phosphate synthase and 3-dehydroquinate synthase, were present, whereas genes with similarity to the two genes for the new pathway were not found. In addition, a transketolase gene, characteristic of the "classical" pathway of biosynthesis of aromatic amino acids, was found in the genome of *I. hospitalis*. All known organisms using the aspartate semialdehyde pathway lack the gene for this enzyme in their genomes (45).

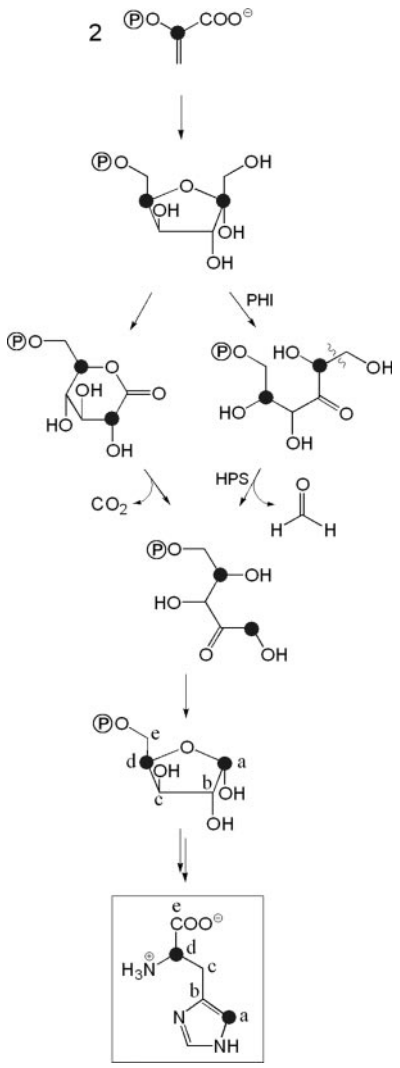

FIG. 4. Biosynthesis of histidine via fructose 6-phosphate from two molecules of PEP. (Left column) Formation of ribulose 5-phosphate by oxidative decarboxylation. (Right column) Formation of ribulose 5-phosphate by the ribulose monophosphate pathway. PHI, 3-hexulose 6-phosphate isomerase; HPS, 3-hexulose 6-phosphate synthase. The circles represent ^{13}C-enriched carbon atoms from [1-^{13}C]acetate. The observed labeling pattern in histidine is shown in the box. The lowercase characters in histidine and ribose phosphate indicate biosynthetically equivalent carbon atoms.

Biosynthesis of lysine may proceed via the common diaminopimelate pathway from pyruvate and aspartate or via the α-aminoadipate pathway, whereby 2-oxoglutarate and acetyl-CoA are condensed and then converted to 2-oxoadipate in much the same way as 2-oxoglutarate is formed in the citric acid cycle (4, 41). The ^{13}C labeling pattern clearly conforms to the second option (Fig. 6).

Biosynthesis of isoleucine via α-ketobutyrate may proceed either via aspartate and threonine or starting from acetyl-CoA and pyruvate (Fig. 7). The detected labeling pattern in isoleucine clearly excludes a biosynthetic pathway via threonine as an intermediate but is perfectly in line with the so-called citramalate pathway via pyruvate (6, 8, 41).

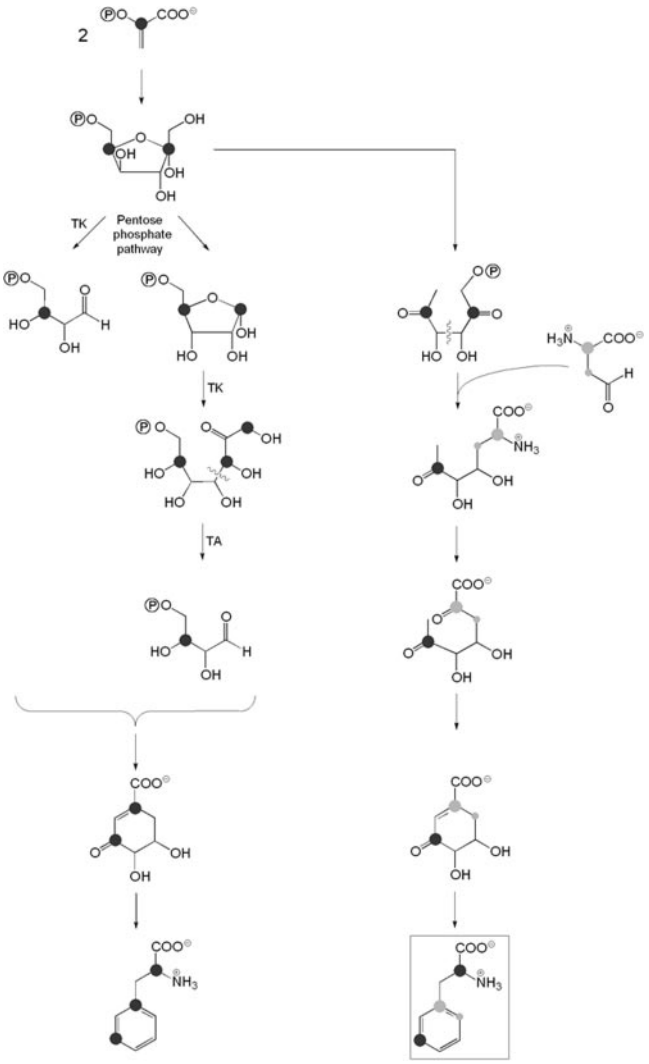

FIG. 5. Biosynthesis of phenylalanine via fructose 6-phosphate. (Left column) Synthesis of erythrose 4-phosphate by reaction of the nonoxidative pentose phosphate pathway. TK, transketolase; TA, transaldolase. The labeling pattern of dehydroshikimate is constructed from erythrose 4-phosphate and PEP on the basis of the conventional shikimate pathway. (Right column) Synthesis via 6-deoxy-5-ketofructose 1-phosphate and aspartate semialdehyde. The labeling pattern of aspartate semialdehyde was predicted from that of aspartate.

DISCUSSION

Evidence for a new autotrophic pathway in *I. hospitalis*. The present work provides substantial arguments in favor of a new autotrophic CO_2 fixation pathway in *I. hospitalis*. RubisCo activity was not detected, nor was the corresponding gene coding for either enzyme form I, II, or III found in the genome. The gene for a RubisCo-like protein was also not seen. Therefore, the Calvin cycle obviously does not work in *I. hospitalis*. The reductive acetyl-CoA pathway is excluded for the same reasons. CO dehydrogenase activity and the genes coding for this enzyme were not found. The citric acid cycle was found to be incomplete, lacking a 2-oxoglutarate-oxidizing enzyme activity. Also, no ATP citrate lyase activity was detected, nor was the corresponding gene found in the genome. In addition, the

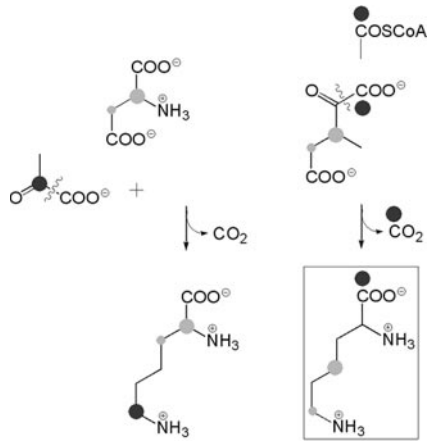

FIG. 6. Biosynthesis of lysine. (Left column) Formation of lysine via the common pathway starting from aspartate and pyruvate and leading to diaminopimelate. (Right column) Formation of lysine via the uncommon pathway starting from 2-oxoglutarate and acetyl-CoA and leading to α-aminoadipate. The circles represent ^{13}C-enriched carbon atoms from [1-^{13}C]acetate. The observed labeling pattern in lysine is shown in the box. The labeling pattern of 2-oxoglutarate is reconstructed from the observed pattern in glutamate, proline, and arginine.

labeling pattern of glutamate proved that C-1 was derived from C-1 of acetyl-CoA rather than from CO_2. The (modified) 3-hydroxypropionate cycle cannot be operative, since acetyl-CoA carboxylase activity was lacking and the corresponding genes were not found, nor could significant amounts of biotin-dependent enzymes be detected in cell extracts. All three criteria

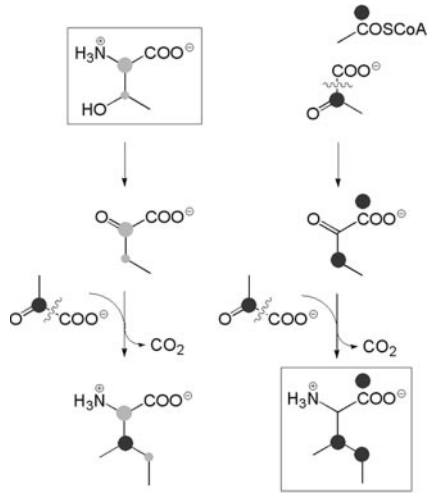

FIG. 7. Biosynthesis of isoleucine. (Left column) Formation of isoleucine via the conventional pathway in which 2-oxobutyrate is formed from threonine. The labeling pattern of threonine corresponds to that of aspartate from which it is formed (Table 3). (Right column) Formation of isoleucine via the unconventional pathway in which 2-oxobutyrate is formed from pyruvate and acetyl-CoA via citramalate and 3-methyloxaloacetate, which is decarboxylated to 2-oxobutyrate. Note that the labeling of 2-oxobutyrate differs in the two pathways. The subsequent steps from 2-oxobutyrate to isoleucine are identical. The circles represent ^{13}C-enriched carbon atoms from [1-^{13}C]acetate. The observed labeling patterns in threonine and isoleucine are shown in boxes. The labeling pattern of pyruvate is reconstructed from the observed pattern in alanine.

were met by *M. sedula*, a member of the *Sulfolobales*, which are postulated to use a modified 3-hydroxypropionate cycle.

Postulated CO_2-fixing enzymes. Extracts contained pyruvate-acceptor oxidoreductase and PEP carboxlase activities. The specific activities at 85°C were approximately 200 nmol min^{-1} mg $protein^{-1}$. The required specific CO_2 fixation rate at a generation time of 2 h is around 400 nmol CO_2 fixed min^{-1} mg $protein^{-1}$. If the new pathway comprises two CO_2 fixation steps, as indicated, the minimal specific enzyme activity of each of the two carboxylating enzymes should be on the order of 200 nmol min^{-1} mg $protein^{-1}$. It should be noted that the enzyme assays have not been optimized and the activity was tested in the direction of pyruvate oxidation with MV as the electron acceptor or by following the incorporation of label from $^{14}CO_2$ into the carboxyl group via the isotope exchange reaction. In growing cells, the reduction of ferredoxin may be brought about by energy-driven reverse electron transport from NAD(P)H, allowing an effective reductive carboxylation of acetyl-CoA (20). The acetate-labeling experiment clearly showed that pyruvate synthase indeed functions in the reductive-carboxylation direction. A similar phenomenon has been observed in *Methanobacterium thermoautotrophicum* strain Marburg (renamed *Methanothermobacter marburgensis*), where acetyl-CoA is converted unidirectionally into pyruvate (11, 46). PEP carboxylation to oxaloacetate by PEP carboxylase is also supported by the labeling pattern of aspartate, where C-4 is derived from CO_2.

Proposed outline of biosynthetic pathways starting from acetyl-CoA. We propose that the autotrophic CO_2 fixation pathway starts from acetyl-CoA. Therefore, we analyzed the assimilation of acetate into cellular building blocks under conditions where 80% of the cell carbon is still derived from CO_2. The observed labeling pattern, together with positive or negative enzyme activity assays and supported by a database search of the genome, are consistent with the following scheme (if not otherwise mentioned, the putative corresponding genes were detected in the genome) (Fig. 1). Acetyl-CoA is reductively carboxylated to pyruvate by pyruvate synthase (see above). Pyruvate is converted into PEP by pyruvate-water dikinase (PEP synthase), and carboxylation of PEP by PEP carboxylase produces oxaloacetate. The citric acid cycle is incomplete and serves only anabolic functions. 2-Oxoglutarate oxidation is missing. Interestingly, the labeling experiments clearly showed that citrate synthase is citrate (re)-synthase (EC 2.3.3.3.) rather than the common (si)-synthase (EC 2.3.3.1.). These two enzymes differ with respect to the side to which acetyl-CoA is added to C-2 of oxaloacetate. They can be discriminated if carbon isotope-labeled acetyl-CoA is used, resulting in chiral citrate (use of unlabeled acetate results in prochiral citrate). Chiral citrate is then converted asymmetrically to 2-oxoglutarate, resulting in differently labeled glutamate. In line with this finding, no citrate (si)-synthase gene was found in the genome.

Gluconeogenesis from PEP appears to be conventional, including a NAD(P)-dependent glyceraldehyde 3-phosphate dehydrogenase. A fructose 1,6-bisphosphate aldolase gene was not detected; however, cell extracts exhibited fructose 1,6-bisphosphate aldolase activity. Fructose 1,6-bisphosphate phosphatase was active in cell extracts, and a putative gene was detected in the genome (see below).

Pentosephosphates are likely derived from hexosephosphate by loss of C-1. The database suggests that this is brought about by enzymes of the ribulose monophosphate pathway (formaldehyde released from C-1) rather than by enzymes of the oxidative pentose phosphate pathway (CO_2 released from C-1).

Catabolic potential. Cultures of *I. hospitalis* cannot grow on sugars (38), and this inability is reflected by the gene outfit and the enzyme pattern. Genes for key enzymes of glycolytic pathways (44) in *Archaea* are apparently not present. These include genes for enzymes of the phosphorylating and nonphosphorylating Entner-Doudoroff pathway and genes encoding glucokinase and phosphofructokinase of a (modified) Embden-Meyerhof pathway, as well as pyruvate kinase and pyruvate dehydrogenase. In accordance with this, neither pyruvate kinase nor pyruvate dehydrogenase activity was detected in cell extracts of *I. hospitalis*. Also, we showed that growing *I. hospitalis* cells are obviously unable to incorporate glucose. Taken together, the data suggest that *I. hospitalis* is unable to gain energy or low-molecular-weight building blocks from oxidizing sugars.

Special enzymes and biosynthetic pathways. The central carbon metabolism of *I. hospitalis* has some special features that are only partly common to *Archaea*. Citrate synthase is (re)-specific. The corresponding gene has not been detected yet; a gene with similarity to (si)-specific citrate synthase is missing, indicating that the re-specific enzyme is completely different. Citrate (re)-synthase has been reported in *Desulfovibrio vulgaris*, *Desulfovibrio desulfuricans*, *Clostridium kluyveri*, *Clostridium acidiurici*, and *Clostridium cylindrosporum* (14–17). The gene for citrate (re)-synthase has been identified as a member of the isopropylmalate synthase enzyme family by expressing the *Ignicoccus* gene in *E. coli* and studying the reaction catalyzed by the enzyme (G. Fuchs and R. Say, unpublished results).

PEP carboxylase is a member of the archaeal-type carboxylase (39). Fructose 1,6-bisphosphate aldolase appears to be different from the known enzyme, since activity was detected but a database search did not yield any hit. Glucose 6-phosphate isomerase seems to be a member of the CUPIN superfamily (18, 19, 47), an archaeal enzyme type that was found in several members of the *Euryarchaeotes*. The new pathway of pentose phosphate synthesis (13, 33, 45), rather than the common oxidative pentose phosphate pathway, seems to be operative, based on the gene outfit and the labeling pattern, which is consistent with this pathway.

Lysine is synthesized via the unconventional α-aminoadipate pathway, rather than via the conventional diaminopimelate pathway. The α-aminoadipate pathway is common in eukaryotes but was also found in *Thermoproteus neutrophilus* within the prokaryotes (42). The biosynthesis of the aromatic amino acids seems to proceed via the shikimate pathway, starting from erythrose 4-phosphate and PEP. Isoleucine is made from α-ketobutyrate, which seems to be assembled from pyruvate and acetyl-CoA but not from threonine. This citramalate pathway (6) is also found in some other *Archaea* (3, 8, 23, 42).

ACKNOWLEDGMENTS

We thank Rafael Say, Freiburg, Germany, for valuable database and literature searches. We thank Christine Schwarz, Garching, Germany, for help with NMR spectroscopy and Fritz Wendling, Garching, Germany, for help with preparation of the manuscript. We acknowledge that the valuable genome database of *I. hospitalis* (http://genome.jgi-psf.org/draft_microbes/ign_k/ign_k.draft.html) was made available to us.

This work was supported by the Deutsche Forschungsgemeinschaft (grant number HU 703/1-2, FU 118/15) and the Fonds der Chemischen Industrie.

REFERENCES

1. **Alber, B., M. Olinger, A. Rieder, D. Kockelkorn, B. Jobst, M. Hügler, and G. Fuchs.** 2006. Malonyl-coenzyme A reductase in the modified 3-hydroxypropionate cycle for autotrophic carbon fixation in archaeal *Metallosphaera* and *Sulfolobus* spp. J. Bacteriol. **188:**8551–8559.
2. **Alber, B. E., and G. Fuchs.** 2002. Propionyl-coenzyme A synthase from *Chloroflexus aurantiacus*, a key enzyme of the 3-hydroxypropionate cycle for autotrophic CO_2 fixation. J. Biol. Chem. **277:**12137–12143.
3. **Bacher, A., C. Rieder, D. Eichinger, D. Arigoni, G. Fuchs, and W. Eisenreich.** 1999. Elucidation of novel biosynthetic pathways and metabolic flux pattern by retrobiosynthetic NMR analysis. FEMS Microbiol. Rev. **22:**567–598.
4. **Bhattacharjee, J. K.** 1985. α-Aminoadipate pathway for the biosynthesis of lysine in lower eukaryotes. Crit. Rev. Microbiol. **12:**131–151.
5. **Bradford, M. M.** 1976. A rapid and sensitive method for the quantitation of microgram quantities of protein utilizing the principle of protein-dye binding. Anal. Biochem. **72:**248–254.
6. **Charon, N. W., R. Johnson, and D. Peterson.** 1974. Amino acid biosynthesis in the spirochete *Leptospira*: evidence for a novel pathway of isoleucine biosynthesis. J. Bacteriol. **117:**203–211.
7. **Dawson, R. M., D. C. Elliot, W. H. Elliot, and K. M. Jones.** 1986. Data for biochemical research, 3rd ed. Clarendon Press, Oxford, United Kingdom.
8. **Eikmanns, B., D. Linder, and R. K. Thauer.** 1983. Unusual pathway of isoleucine biosynthesis in *Methanobacterium thermoautotrophicum*. Arch. Microbiol. **136:**111–113.
9. **Eisenreich, W., and A. Bacher.** 2000. Elucidation of biosynthetic pathways by retrodictive/predictive comparison of isotopomer patterns determined by NMR spectroscopy. Genet. Eng. **22:**121–153.
10. **Eisenreich, W., B. Schwarzkopf, and A. Bacher.** 1991. Biosynthesis of nucleotides, flavins, and deazaflavins in *Methanobacterium thermoautotrophicum*. J. Biol. Chem. **266:**9622–9631.
11. **Fuchs, G., and E. Stupperich.** 1980. Acetyl-CoA, a central intermediate of autotrophic CO_2 fixation in *Methanobacterium thermoautotrophicum*. Arch. Microbiol. **127:**267–272.
12. **Gallagher, S., S. E. Winston, S. A. Fuller, and J. G. R. Hurrell.** 1997. Immunoblotting and immunodetection, p. 10.8.1–10.8.21. *In* F. M. Ausubel et al. (ed.), Current protocols in molecular biology. John Wiley & Sons, Inc., New York, NY.
13. **Goenrich, M., R. K. Thauer, H. Yurimoto, and N. Kato.** 2005. Formaldehyde activating enzyme (Fae) and hexulose-6-phosphate synthase (Hps) in *Methanosarcina barkeri*: a possible function in ribose-5-phosphate biosynthesis. Arch. Microbiol. **184:**41–48.
14. **Gottschalk, G.** 1968. The stereospecificity of the citrate synthase in sulfate-reducing and photosynthetic bacteria. Eur. J. Biochem. **5:**346–351.
15. **Gottschalk, G.** 1969. Partial purification and some properties of the (*R*)-citrate synthase from *Clostridium acidiurici*. Eur. J. Biochem. **7:**301–306.
16. **Gottschalk, G., and H. A. Barker.** 1966. Synthesis of glutamate and citrate by *Clostridium kluyveri*. A new type of citrate synthase. Biochemistry **5:**1125–1133.
17. **Gottschalk, G., and H. A. Barker.** 1967. Presence and stereospecificity of citrate synthase in anaerobic bacteria. Biochemistry **6:**1027–1034.
18. **Hansen, T., M. Oehlmann, and P. Schönheit.** 2001. Novel type of glucose-6-phosphate isomerase in the hyperthermophilic archaeon *Pyrococcus furiosus*. J. Bacteriol. **183:**3428–3435.
19. **Hansen, T., B. Schlichting, M. Felgendreher, and P. Schönheit.** 2005. Cupin-type phosphoglucose isomerases (Cupin-PGIs) constitute a novel metal-dependent PGI family representing a convergent line of PGI evolution. J. Bacteriol. **187:**1621–1631.
20. **Hedderich, R.** 2004. Energy-converting [NiFe] hydrogenases from archaea and extremophiles: ancestors of complex I. J. Bioenerg. Biomembr. **36:**65–75.
21. **Herter, S., J. Farfsing, N. Gad'On, C. Rieder, W. Eisenreich, A. Bacher, and G. Fuchs.** 2001. Autotrophic CO_2 fixation by *Chloroflexus aurantiacus*: study of glyoxylate formation and assimilation via the 3-hydroxypropionate cycle. J. Bacteriol. **183:**4305–4316.
22. **Howard, J. L., and S. M. Ridley.** 1990. Acetyl-CoA carboxylase: a rapid novel assay procedure used in conjunction with the preparation of enzyme from maize leaves. FEBS Lett. **261:**261–264.
23. **Howell, D. M., H. Xu, and R. H. White.** 1999. (*R*)-citramalate synthase in methanogenic archaea. J. Bacteriol. **181:**331–333.
24. **Huber, H., S. Burggraf, T. Mayer, I. Wyschkony, R. Rachel, and K. O. Stetter.** 2000. *Ignicoccus* gen. nov., a novel genus of hyperthermophilic, chemolithoautotrophic *Archaea*, represented by two new species, *Ignicoccus islandicus* sp. nov. and *Ignicoccus pacificus* sp. nov. Int. J. Syst. Evol. Microbiol. **50:**2093–2100.
25. **Huber, H., M. J. Hohn, R. Rachel, T. Fuchs, V. C. Wimmer, and K. O. Stetter.** 2002. A new phylum of Archaea represented by a nanosized hyperthermophilic symbiont. Nature **417:**63–67.
26. **Huber, H., M. J. Hohn, K. O. Stetter, and R. Rachel.** 2003. The phylum Nanoarchaeota: present knowledge and future perspectives of a unique form of life. Res. Microbiol. **154:**165–171.
27. **Huber, G., C. Spinnler, A. Gambacorta, and K. O. Stetter.** 1989. *Metallosphaera sedula*, gen. and sp. nov. represents a new genus of aerobic, metal-mobilizing, thermoacidophilic archaebacteria. Syst. Appl. Microbiol. **12:**38–47.
28. **Hügler, M., H. Huber, K. O. Stetter, and G. Fuchs.** 2003. Autotrophic CO_2 fixation pathways in archaea (Crenarchaeota). Arch. Microbiol. **179:**160–173.
29. **Hügler, M., C. Menendez, H. Schägger, and G. Fuchs.** 2002. Malonyl-coenzyme A reductase from *Chloroflexus aurantiacus*, a key enzyme of the 3-hydroxypropionate cycle for autotrophic CO_2 fixation. J. Bacteriol. **184:**2404–2410.
30. **Hügler, M., C. O. Wirsen, G. Fuchs, C. D. Taylor, and S. M. Sievert.** 2005. Evidence for autotrophic CO_2 fixation via the reductive tricarboxylic acid cycle in members of the ε-*Proteobacteria*. J. Bacteriol. **187:**3020–3027.
31. **Imanaka, H., A. Yamatsu, T. Fukui, H. Atomi, and T. Imanaka.** 2006. Phosphoenol-pyruvate synthase plays an essential role for glycolysis in the modified Embden-Meyerhof pathway in *Thermococcus kodakarensis*. Mol. Microbiol. **61:**898–909.

31a. **Ishii, M., T. Miyake, T. Satoh, H. Sugiyama, Y. Oshima, T. Kodama, and Y. Igarashi.** 1996. Autotrophic carbon dioxide fixation in *Acidianus brierleyi*. Arch. Microbiol. **166:**368–371.

32. **Jahn, U., R. Summons, H. Sturt, E. Grosjean, and H. Huber.** 2004. Composition of the lipids of *Nanoarchaeum equitans* and their origin from its host *Ignicoccus* sp. strain KIN4/I. Arch. Microbiol. **182:**404–413.
33. **Kato, N., H. Yurimoto, and R. K. Thauer.** 2006. The physiological role of the ribulose monophosphate pathway in bacteria and archaea. Biosci. Biotechnol. Biochem. **70:**10–21.
34. **Madigan, M., and J. Martinko.** 2006. Brock biology of microorganisms, 11th ed. Prentice Hall, Upper Saddle River, NJ.
35. **Menendez, C., Z. Bauer, H. Huber, N. Gad'on, K. O. Stetter, and G. Fuchs.** 1999. Presence of acetyl coenzyme A (CoA) carboxylase and propionyl-CoA carboxylase in autotrophic Crenarchaeota and indication for operation of a 3-hydroxypropionate cycle in autotrophic carbon fixation. J. Bacteriol. **181:**1088–1098.
36. **Mukhopadhyay, B., V. J. Patel, and R. S. Wolfe.** 2000. A stable archaeal pyruvate carboxylase from the hyperthermophile *Methanococcus jannaschii*. Arch. Microbiol. **174:**406–414.
37. **Mukhopadhyay, B., and E. Purwantini.** 2000. Pyruvate carboxylase from *Mycobacterium smegmatis*: stabilization, rapid purification, molecular and biochemical characterization and regulation of the cellular level. Biochim. Biophys. Acta **1475:**191–206.
38. **Paper, W., U. Jahn, M. J. Hohn, M. Brandl, D. J. Näther, T. Burghardt, R. Rachel, K. O. Stetter, and H. Huber.** 2007. *Ignicoccus hospitalis* sp. nov., the host of *Nanoarchaeum equitans*. Int. J. Syst. Evol. Microbiol. **57:**803–808.
39. **Patel, H. M., J. L. Kraszewski, and B. Mukhopadhyay.** 2004. The phosphoenol-pyruvate carboxylase from *Methanothermobacter thermoautotrophicus* has a novel structure. J. Bacteriol. **186:**5129–5137.
40. **Rachel, R., I. Wyschkony, S. Riehl, and H. Huber.** 2002. The ultrastructure of *Ignicoccus*: evidence for a novel outer membrane and for intracellular vesicle budding in an archaeon. Archaea **1:**9–18.
41. **Schäfer, S., M. Gotz, W. Eisenreich, A. Bacher, and G. Fuchs.** 1989. ^{13}C-NMR study of autotrophic CO_2 fixation in *Thermoproteus neutrophilus*. Eur. J. Biochem. **184:**151–156.
42. **Schäfer, S., T. Paalme, R. Vilu, and G. Fuchs.** 1989. ^{13}C-NMR study of acetate assimilation in *Thermoproteus neutrophilus*. Eur. J. Biochem. **186:**695–700.
43. **Selkov, E., N. Maltsev, G. J. Olsen, R. Overbeek, and W. B. Whitman.** 1997. A reconstruction of the metabolism of *Methanococcus jannaschii* from sequence data. Gene **197:**GC11–GC26.
44. **Siebers, B., and P. Schönheit.** 2005. Unusual pathways and enzymes of central carbohydrate metabolism in Archaea. Curr. Opin. Microbiol. **8:**695–705.
45. **Soderberg, T.** 2005. Biosynthesis of ribose-5-phosphate and erythrose-4-phosphate in archaea: a phylogenetic analysis of archaeal genomes. Archaea **1:**347–352.
46. **Tersteegen, A., D. Linder, R. K. Thauer, and R. Hedderich.** 1997. Structures and functions of four anabolic 2-oxoacid oxidoreductases in *Methanobacterium thermoautotrophicum*. Eur. J. Biochem. **244:**862–868.
47. **Verhees, C. H., M. A. Huynen, D. E. Ward, E. Schiltz, W. M. de Vos, and J. van der Oost.** 2001. The phosphoglucose isomerase from the hyperthermophilic archaeon *Pyrococcus furiosus* is a unique glycolytic enzyme that belongs to the cupin superfamily. J. Biol. Chem. **276:**40926–40932.
48. **Waters, E., M. J. Hohn, I. Ahel, D. E. Graham, M. D. Adams, M. Barnstead, K. Y. Beeson, L. Bibbs, R. Bolanos, M. Keller, K. Kretz, X. Lin, E. Mathur, J. Ni, M. Podar, T. Richardson, G. G. Sutton, M. Simon, D. Soll, K. O. Stetter, J. M. Short, and M. Noordewier.** 2003. The genome of *Nanoarchaeum equitans*: insights into early archaeal evolution and derived parasitism. Proc. Natl. Acad. Sci. USA **100:**12984–12988.
49. **White, R. H.** 2004. L-Aspartate semialdehyde and a 6-deoxy-5-ketohexose 1-phosphate are the precursors to the aromatic amino acids in *Methanocaldococcus jannaschii*. Biochemistry **43:**7618–7627.
50. **Yu, J. P., J. Ladapo, and W. B. Whitman.** 1994. Pathway of glycogen metabolism in *Methanococcus maripaludis*. J. Bacteriol. **176:**325–332.